Polymerized Rodlike Nanoparticles with Controlled Surface Charge Density

ARTICLE *in* LANGMUIR · APRIL 2006

Impact Factor: 4.46 · DOI: 10.1021/la052949a · Source: PubMed

3 AUTHORS, INCLUDING:

Tae-Hwan Kim
Korea Atomic Energy Research Institute (KAE…

31 PUBLICATIONS **241** CITATIONS

SEE PROFILE

Polymerized Rodlike Nanoparticles with Controlled Surface Charge Density

Tae-Hwan Kim,[†] Sung-Min Choi,*[,†] and Steven R. Kline[‡]

Department of Nuclear and Quantum Engineering, Korea Advanced Institute of Science and Technology, 373−1 Guseong-dong, Yuseong-gu, Daejeon, 305-701 Korea, and NIST Center for Neutron Research, Gaithersburg, Maryland 20899-8562

Received November 2, 2005. In Final Form: January 18, 2006

Stable rodlike nanoparticles with highly controlled surface charge density have been developed by the free radical polymerization of the mixture of polymerizable cationic surfactant, cetyltrimethylammonium 4-vinylbenzoate (CTVB), and hydrotropic salt sodium 4-styrenesulfonate (NaSS) in aqueous solution. The surface charge of the polymerized CTVB/NaSS rodlike nanoparticles was controlled by varying the NaSS concentration during the polymerization process, and the charge variation was interpreted in terms of the overcharging effect in colloidal systems. The SANS measurements show that the diameter of the polymerized CTVB/NaSS rodlike nanoparticles is constant at 4 nm and the particle length ranges from 24 to 85 nm, depending on the NaSS concentration. The polymerized particles are longest when the NaSS concentration is 5 mol % which corresponds to the charge inversion or neutral point. The SANS and zeta potential measurements show that the Coulomb interactions between the particles are strongly dependent on the NaSS concentration and the zeta potential of the polymerized CTVB/NaSS nanoparticles changes from positive to negative (+12.8 ∼ −44.2 mV) as the concentration of NaSS increases from 0 to 40 mol %. As the NaSS concentration is further increased, the zeta potential is saturated at approximately −50 mV.

Introduction

Surfactant molecules in aqueous solution show fascinating phase behavior and self-assemble into various micellar structures such as spheres, cylinders, vesicles or lamellae above the critical micellar concentration (cmc).[1,2] Therefore, the self-assembled molecular aggregates have been very popular as templates for preparing various nanostructured materials such as nanoclusters, nanocrystals, and nanorods.[3,4] However, due to their dynamic nature, micellar structures are very sensitive to solution conditions such as temperature, concentration, pH, and pressure[5−11] and are easily transformed from one structure to another, limiting their applications.

Polymerization of surfactants as a means of "locking in" the molecular self-assembling architectures leads to the formation of the stable nanostructures that are insensitive to environmental changes and could provide a basis for novel applications.[3,12] Recently, this approach has attracted great interest,[13−15] and the polymerization of self-assembled surfactant or block copolymer systems such as spherical or cylindrical micelles,[16−22] vesicles,[23,24] lyotropic liquid crystals,[25] and microemulsions[26] have been studied by various groups.

Recently, Kline,[27] one of the authors of this paper, reported a new cationic surfactant cetyltrimethylammonium 4-vinylbenzoate (CTVB) that has a polymerizable counterion. The CTVB molecules in water form viscoelastic wormlike micelles, and upon free-radical polymerization of the counterions, they transform into nanoparticles that remain well dispersed in water. Small-angle neutron scattering (SANS) measurements showed that the resulting nanoparticles are cylindrical in shape with diameter of 4 nm and length of 96∼240 nm depending on the relative concentration of the polymerization initiator.[28] The polymerized cylindrical nanoparticles are remarkably stable against temperature or dilution and redispersible in water after freeze-drying, which is in sharp contrast to unpolymerized surfactant systems. To utilize the polymerized rodlike particles for various applications, however, it would be advantageous to have control of the surface properties of the particles.

In this paper, we report a novel method of preparing stable charged rodlike nanoparticles with well-controlled surface charge

* To whom correspondence should be addressed. E-mail: sungmin@kaist.ac.kr.

† Korea Advanced Institute of Science and Technology.

‡ NIST Center for Neutron Research.

(1) Israelachvili, J. N. *Intermolecular and Surface Forces*; Academic Press: New York, 1992.
(2) Hiemenz, P. C.; Rajagopalan, R. *Principles of Colloid and Surface Chemistry*, 3rd ed.; Marcel Dekker: New York, 1997.
(3) Paleos, C. M. In *Polymerization in Organized Media*; Paleos, C. M., Ed.; Gordon and Beach: Philadelphia, 1992.
(4) Cao, G. *Nanostructures and Nanomaterials*; Imperial College Press: London, 2004.
(5) Kakitani, M.; Imae, T.; Furusaka, M. *J. Phys. Chem.* **1995**, *99*, 16018.
(6) Heindl, A.; Kohler, H. H. *Langmuir* **1996**, *12*, 2464.
(7) Hassan, P. A.; Fritz, G.; Kaler, E. W. *J. Colloid Interface Sci.* **2003**, *57*, 154.
(8) Aswal, V. K.; Goyal, P. S. *Chem. Phys. Lett.* **2002**, *364*, 44.
(9) Heerklotz, H.; Tsamaloukas, A.; Kita-tokarczyk, K.; Strunz, P.; Gutberlet, T. *J. Am. Chem. Soc.* **2004**, *126*, 16544.
(10) Schurtenberger, R.; Cavaco, C. *Langmuir* **1996**, *12*, 2894.
(11) Aswal, V. K.; Goyal, P. S. *Chem. Phys. Lett.* **2002**, *357*, 491.
(12) Pendler, J. H.; Tundo, P. *Acc. Chem. Res.* **1984**, *17*, 3.
(13) Tajima, K.; Aida, T. *Chem. Commun.* **2000**, *24*, 2399.
(14) Summers, M.; Eastoe, J. *Adv. Colloid Interface Sci.* **2003**, *100−102*, 137.
(15) Seth, A. M.; Ding, J. H.; Gin, D. L. *Curr. Opin. Colloid Interface Sci.* **1998**, *4*, 338.
(16) Büün, V.; Billingham, N. C.; Armes, S. P. *J. Am. Chem. Soc.* **1998**, *120*, 12135.
(17) Thurmond, K. B., II; Kowalewski, T.; Wooley, K. L. *J. Am. Chem. Soc.* **1996**, *118*, 7239.
(18) Ding, J.; Liu, G. *Macromolecules* **1998**, *31*, 6554.
(19) Hamid, S. M.; Sherrington, D. C. *Polymer* **1987**, *28*, 332.
(20) Dufour, M.; Guyot, A. *Colloid Polym. Sci.* **2003**, *281*, 97.
(21) Summers, M.; Eastoe, J.; Davis, S.; Du, Z.; Richardson, R. M.; Heenan, R. K.; Steytler, D.; Grillo, I. *Langmuir* **2001**, *17*, 5388.
(22) Percec, V.; Ahn, C. H.; Barboiu, B. *J. Am. Chem. Soc.* **1997**, *119*, 12978.
(23) Regen, S. L.; Czech, B.; Singh, A. *J. Am. Chem. Soc.* **1980**, *102*, 6638.
(24) Mckelvey, C. A.; Kaler, E. W.; Zasadzinski, J. A.; Coldren, B.; Jung, H. T. *Langmuir* **2000**, *16*, 8285.
(25) Gin, D. L.; Gu, W.; Pindzola, B. A.; Zhou, W. *Acc. Chem. Res.* **2001**, *34*, 973.
(26) Fu, X.; Qutubuddin, S. *Langmuir* **2002**, *18*, 5058.
(27) Kline, S. R. *Langmuir* **1999**, *15*, 2726.
(28) Gerber, M. J.; Kline, S. R.; Walker, L. M. *Langmuir* **2004**, *20*, 8510.

10.1021/la052949a CCC: $33.50
Published on Web 02/15/2006

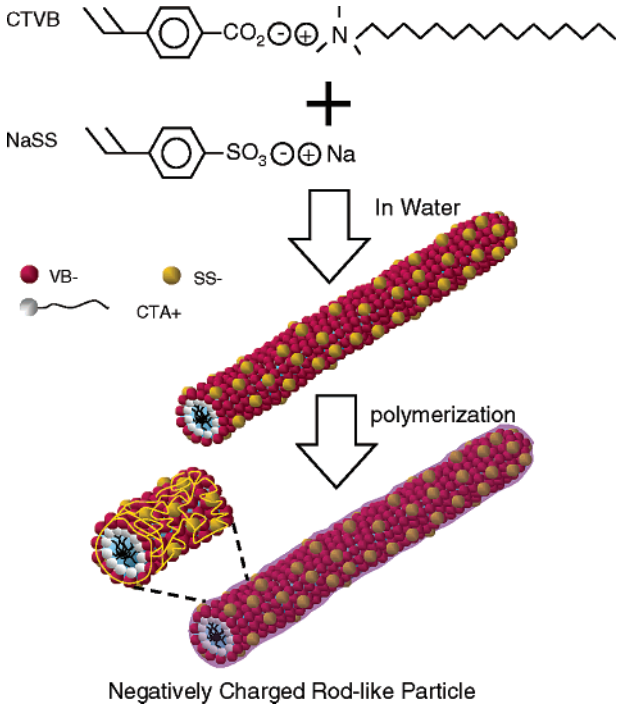

Figure 1. Schematic of surface charge control. The polymerizable counterions VB^- and SS^- are closely associated with CTA^+ ions and are copolymerized, increasing the surface charge density of polymerized CTVB. The surface of polymerized CTVB was overcharged by SS^- ions.

density using a mixture of CTVB and sodium 4-styrenesulfonate (NaSS) in aqueous solution. Figure 1 schematically shows the basic concept of the method that involves the free-radical polymerization of the counterions (VB^-, ions of CTVB; SS^-, ions of NaSS) of wormlike micelles. Here, the surface charge density of the polymerized particles is controlled by varying the concentration of NaSS, i.e., overcharging the micelles by polymerizable anions. With only CTVB present, some small number of unpolymerized VB^- ions can dissociate from the surface of the wormlike micelles, giving the micelle a positive charge. When there is SS^- present, the Na^+ ions dissociate much more freely, and there are many more of them than any residual VB^-. All of these extra SS^- ions on the surface of micelle cancel out the positive charge and lead to a net negative charge at higher SS^- concentrations. When the wormlike micelles overcharged by SS^- ions are polymerized, they become the negatively charged stable rodlike nanoparticles. SANS, dynamic light scattering (DLS), and zeta potential measurements were used to characterize the morphology and surface charge properties of the polymerized CTVB/NaSS nanoparticles in dilute and concentrated solutions. To our knowledge, this is the first attempt to fabricate highly anisotropic nanoparticles with controlled surface charge density using polymerization and the overcharging effect in colloidal systems.

Experimental Section

Cetyltrimethylammonium hydroxide (CTAOH) and sodium 4-styrenesulfonate (NaSS) were purchased from Fluka. 4-Vinylbenzoic acid was purchased from Aldrich. D_2O (99.9 mol % deuterium enriched) was purchased from Cambridge Isotope Laboratory. The water-soluble free-radical initiator VA-044 (2,2′-azobis[2-(2-imidazolin-2-yl)propane] dihydrochloride) was purchased from Wako Chemicals. H_2O was purified by Millipore Direct Q system immediately before use.[29]

Cetyltrimethylammonium 4-vinylbenzoate (CTVB) was synthesized by neutralization of 4-vinylbenzoic acid in the presence of a slight stoichiometric excess of CTAOH followed by repeated crystallization.[27]

The critical micellar concentration was determined from electrical conductivity measurements using the WTW conductivity cell (model TetraCon 325) with a cell constant 0.475 cm^{-1}.

For the counterion polymerization of CTVB, 1 wt % of CTVB solution was prepared using water in which oxygen was depleted by bubbling with ultrahigh purity nitrogen. The solution was shaken for about 12 h for complete dissolution. The solution was very viscoelastic indicating the formation of long, entangled rodlike micelles. While maintaining the temperature at 60 °C, 5 mol % (relative to the CTVB concentration) of the initiator VA-044 (prepared in 1 mL of oxygen depleted water) was injected into the 1 wt % CTVB solution using a syringe. The syringe was flushed with nitrogen gas before use to remove residual oxygen. Right after the injection of initiator, the CTVB solution was vigorously shaken and then put into to a thermal bath at 60 °C.

To control the surface charge density of the polymerized CTVB, varying amounts (0, 5, 10, 25, 40, 50, and 60 mol % relative to the CTVB concentration) of NaSS was dissolved into the CTVB solution before injecting the initiator. Upon completion of the polymerization process, all of the samples were freeze-dried for 3 days. The dried samples were readily re-dispersible in water and used to prepare samples of various concentrations.

To verify the counterion polymerization of CTVB, NMR measurements were carried out on a Bruker FT-500 MHz NMR spectrometer. For these measurements, all samples were dissolved in D_2O.

The surface charge densities of polymerized CTVB with different amounts of NaSS were characterized by zeta potential measurements using a ZetaPlus zeta potential analyzer (Brookhaven Instruments Corporation). The zeta potential was calculated by the Smoluchowski's equation via the measurement of the electrophoretic mobility. The hydrodynamic radii of 0.1 wt % polymerized CTVB/NaSS particles in D_2O were estimated from dynamic light scattering (DLS) measurements ($\lambda = 659$ nm, scattering angle = 90°) using a ZetaPlus particle size analyzer (Brookhaven Instruments Corporation).

The viscosity measurements for the CTVB solutions were carried out using a Cannon-Fenske capillary viscometer.

Small-angle neutron scattering (SANS) measurements were performed to characterize the structures and the effects of NaSS on the surface charge of the polymerized CTVB. SANS experiments were carried out on the NG3 30m SANS instrument at the National Institute of Standard and Technology (NIST) in Gaithersburg, MD and on the 9m SANS instrument at High-flux Advanced Neutron Application Reactor (HANARO) in Korea Atomic Energy Research Institute (KAERI), Korea. In the experiments at NIST, neutrons of wavelength $\lambda = 6.5$ Å with full width half-maximum $\Delta\lambda/\lambda = 10\%$ were used. Two different sample to detector distances (1.3 m and 13 m) were used to cover the overall q range of 0.0035 $Å^{-1} < q <$ 0.4183 $Å^{-1}$ where $q = (4\pi/\lambda)\sin(\theta/2)$ is the magnitude of the scattering vector and θ is the scattering angle. Sample scattering was corrected for background and empty cell scattering, and the sensitivity of individual detector pixels. The corrected data sets were placed on an absolute scale using standard samples and data reduction software provided by NIST.[30] In the experiments at HANARO, neutrons of wavelength $\lambda = 5.08$ Å with full width half-maximum $\Delta\lambda/\lambda = 11.8\%$ were used. One sample to detector distance (3 m) was used to cover the q range of 0.01 $Å^{-1} < q <$ 0.2488 $Å^{-1}$ to confirm the temperature insensitivity of polymerized CTVB/NaSS particles.

Data Analysis. SANS data sets were analyzed by the methods as follows: Guinier fitting, rigid cylindrical form factor fitting with and without considering the screened Coulomb interaction structure factor. For a very dilute colloidal system, the scattering intensity can be approximated in the $qR_g < 1$ region

(29) The use of specific trade names does not imply endorsement of products or companies by NIST but are used to fully describe the experimental procedures.

(30) *NIST SANS Data Reduction and Imaging Software*, 2003.

$$\ln I(q) = \ln I(0) - \frac{1}{3}q^2R_g^2 \quad (1)$$

where R_g is the radius of gyration of particles. For a cylindrical particle, R_g is related to the radius R and the length L as

$$R_g^2 = \frac{R^2}{2} + \frac{L^2}{12} \quad (2)$$

If the radius of the cylindrical particle is known from other measurements or analysis, the length can be estimated from R_g using eq 2, which is the case in our study. For very dilute solutions of particles where the interparticle interactions are negligible, the scattering intensity can be simplified as

$$I(q) = nP(q) + b \quad (3)$$

where n is the number density of particles, $P(q)$ is the intraparticle interference (called the form factor) averaged over a Schulz distribution[31] of cylinder length, and b is the residual incoherent scattering. The Schulz width parameter is given as $z = 1/p_L^2 - 1$, where p_L is the polydispersity ($=\sigma_L/L$). The form factor for the rigid cylinder particles is given as[32−34]

$$P(q) = \int_0^{\pi/2} f^2(q,\alpha) \sin \alpha \, d\alpha$$

$$f(q,\alpha) = 2(\rho_{cyl} - \rho_{solv})Vj_0\left(\frac{qL\cos\alpha}{2}\right)\frac{J_1(qR\sin\alpha)}{(qR\sin\alpha)}$$

$$j_0 = \sin(x)/x \quad (4)$$

where V is the volume of the particle and, ρ_{cyl} and ρ_{solv} are scattering length densities of the particles and solvent, respectively. $J_1(x)$ is the first-order Bessel function and α is the angle between the cylinder axis and the scattering vector, q.

When the interparticle interactions are not negligible, the scattering intensity can be written as

$$I(q) = nP(q)S(q) + b \quad (5)$$

where $S(q)$ is the interparticle interference (called the structure factor) for which we used the rescaled mean spherical approximation (MSA) screened Coulomb interaction structure factor.[35,36] Since the rescaled MSA screened Coulomb interaction structure factor is for spherical particle, the effective diameters (D_{eff}) of the cylindrical particles, which were calculated by a method proposed by Isihara,[37] were used in the model fitting. The effective diameter in terms of the particle length L and the particle radius R is given as

$$\frac{4}{3}\pi(D_{eff}/2)^3 = \pi R^2 L f \quad (6)$$

where $f = 1/4(1 + L/2R(1 + R/L)(1 + \pi R/L))$. In the model fits, the Debye screening length was calculated using the concentrations of Na^+ and free (not incorporated into the polymerized aggregates) SS^- and VB^- ions. The concentrations of free SS^- and VB^- ions are coupled with the surface charge density of particles, one of the fitting parameters.

Result and Discussion

The identity of prepared CTVB surfactants was confirmed by NMR measurements in D_2O, and all of the peaks in the NMR spectrum correspond to the reference spectra.[38] The cmc of CTVB in aqueous solution, measured by electrical conductivity, was 0.0076 wt % and was consistent with the previous work.[27] Also, the polymerizable surfactant CTVB formed wormlike micelles in aqueous solution and 1 wt % CTVB in water was very viscoelastic.[27] Upon polymerization of counterions around the wormlike micelles, the viscosity of solution was dramatically reduced from ~420 to ~1.5 cP and became fluid with a waterlike viscosity. This may indicate that the polymerization does not capture the whole entangled wormlike micellar structures but captures only the local structures producing shorter cylindrical particles.

To control the surface charge density of the polymerized CTVB nanoparticles, various amounts (0, 5, 10, 25, 40, 50, and 60 mol % relative to the CTVB concentration) of NaSS were added into 1 wt % CTVB aqueous solution before free-radical polymerization. Due to its negative charge and hydrophobic nature, the polymerizable SS^- ions are distributed on the surface of wormlike micelles along with the polymerizable VB^- ions of CTVB. In this process, the wormlike micelles can be negatively charged by overcharging effect.[39−42] The surface charge density of the wormlike micelle can be controlled by the amount of NaSS added.

The wormlike micelles of CTVB and NaSS mixture solutions were polymerized by injecting 5 mol % (relative to the CTVB concentration) of VA-044 at 60 °C. The temperature was maintained until the polymerization was completed. The progress of the polymerization reactions were followed visually, which were slightly different depending on the concentration of NaSS. When no NaSS was added, the solution initially became bluish for few minutes and then cloudy for about 20 min. After this, the solution eventually became transparent and, unlike its parent solution, very fluid without any viscoelasticity. When 10 mol % NaSS was added, the solution became very cloudy within a few minutes and phase separated after about 30 min, with milky aggregates on the top and transparent and fluid solution at the bottom. The proportion of milky aggregates decreased with time and completely disappeared within 12 h, resulting in a transparent and fluid solution. The proportion of the milky aggregates depended on the concentration of NaSS, largest at 5 mol % and smallest at 40 mol %. All polymerized solutions became transparent after 12 h and remained stable indefinitely.

The conversion of counterions to polymer was verified by NMR measurements. Figure 2 shows the proton NMR spectra of unpolymerized and polymerized CTVB and NaSS mixtures in D_2O. In these measurements, the concentration of NaSS was 40 mol % relative to the CTVB concentration. The spectrum of the unpolymerized CTVB and NaSS mixture is nearly identical to that of unpolymerized CTVB because the NaSS molecules have the same aromatic group and vinyl group as VB^- ions. The NMR spectrum of NaSS in D_2O is shown in the inset of Figure 2b, which is very similar to the reference spectrum of VBA. The NMR spectrum of the unpolymerized CTVB and NaSS mixture is shown in Figure 2a, and the peaks correspond to the protons in the alkyl chain group (1.03 and 1.43 ppm), the 3 methyl groups

(31) Schulz, G. V. *Z. Phys. Chem. Abt. B* **1939**, *43*, 25.
(32) Guinier, A.; Fournet, G. *Small-Angle Scattering of X-Rays*; John Wiley and Sons: New York, 1955.
(33) Feigin, L. A.; Svergun, D. I. In *Structure Analysis by Small-Angle X-ray and Neutron Scattering*; Taylor, G. W., Ed.; Plenum Press: New York, 1987.
(34) Higgins, J. S.; Benoit, H. C. *Polymers and Neutron Scattering*; Oxford University Press: New York, 1994.
(35) Hayter, J. B.; Penfold, J. *Mol. Phys.* **1981**, *42*, 109.
(36) Hansen, J. P.; Hayter, J. B. *Mol. Phys.* **1982**, *46*, 651.
(37) Isihara, A. *J. Chem. Phys.* **1950**, *18*, 1446.
(38) *The Aldrich library of NMR spectra*, 2nd ed.; Aldrich Chemical Co.: Milwaukee, WI, 1983.
(39) Martin-Molina, A.; Quesada-Perez, M.; Galisteo-Gonzalez, F.; Hidalgo-Alvarez, R. *J. Phys.: Condens. Matter* **2003**, *15*, S3475.
(40) Messina, R.; C. Holm, C.; Kremer, K. *Phys. Rev. E* **2001**, *64*, 021405.
(41) Park, S. Y.; Bruinsma, R. F.; Gelbart, W. M. *Europhys. Lett.* **1999**, *46*, 454.
(42) Mateescu, E. M.; Jeppesen, C.; Pincus, P. *Europhys. Lett.* **1999**, *46*, 493.

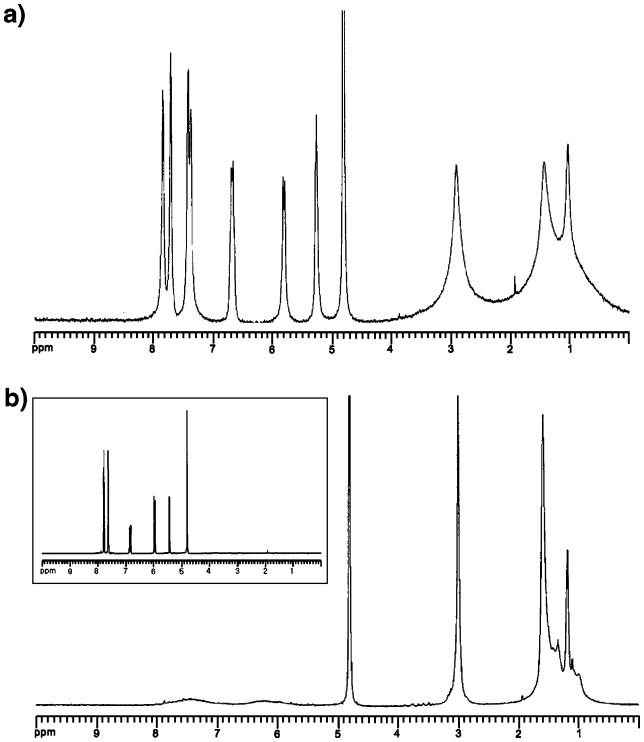

Figure 2. (a) Proton NMR spectrum of unpolymerized CTVB with NaSS 40 mol %. (b) Proton NMR spectrum of polymerized CTVB with NaSS 40 mol %. The small picture is the proton NMR spectrum of NaSS only. The vinyl signal disappears during polymerization, and the aromatic group signal loss is the result of a drastic change in molecular mobility of the counterions after copolymerization relative to the NMR time scale.

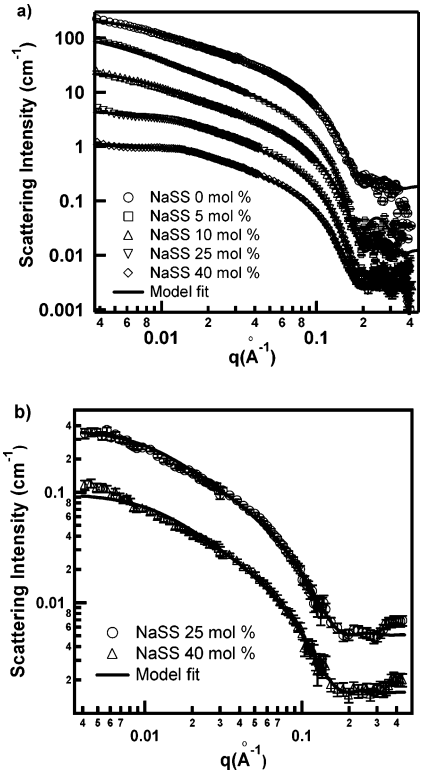

Figure 3. SANS intensities of polymerized CTVB in D_2O with varying NaSS concentrations. The solid lines are model fitting with a cylindrical form factor. For the length of the cylinder the Schulz distribution is assumed. (a) 0.1 wt % polymerized CTVB in D_2O. The intensities of NaSS 0 (×100), 5 (×25), 10 (×10), and 25 (×3) mol % are vertically shifted for visual clarity. (b) 0.01 wt % polymerized CTVB in D_2O (0.047 M NaCl). The intensity of NaSS 25 mol % (×3) is vertically shifted.

coupled with nitrogen (2.91 ppm), residual H_2O (4.8 ppm), the vinyl group (5.26, 5.79, 5.82, 6.64, 6.66, and 6.69 ppm), and the aromatic group (7.37, 7.42, 7.70, and 7.84 ppm). The NMR spectrum of polymerized CTVB and NaSS mixture is shown in Figure 2b. The peaks arising from the vinyl groups have completely disappeared upon polymerization, indicating a very high degree of conversion of the monomer. It should be noted that the peaks of the aromatic groups of the counterions VB^- and SS^- disappear after polymerization. Upon polymerization, the mobility of the counterions is dramatically reduced, and hence, the T2-relaxation time of aromatic and vinyl groups becomes very short, resulting in almost complete disappearance of corresponding peaks. This, therefore, clearly indicates that both of the counterions VB^- and SS^- are incorporated into the polymerization. It is also noticeable that the line width of the peaks corresponding to the alkyl chain group and the three methyl groups coupled with nitrogen becomes much sharper upon polymerization, which is a result of the dramatically reduced viscosity after polymerization.

The structures of polymerized CTVB particles, which were copolymerized with various amounts of NaSS, were characterized by SANS measurements. The SANS intensities of 0.1 wt % polymerized CTVB/NaSS particles in D_2O are shown in Figure 3a. Since the sample concentration is very dilute, the effects of interparticle interaction are expected to be very small. However, since the low q region, which contains the length information of the rodlike particles, is very sensitive to the interparticle interaction, we analyzed the data using the cylindrical form factor with and without considering the screened Coulomb interaction structure factor. The lengths and radii of rodlike particles obtained with and without considering the interparticle interaction are essentially identical. Therefore, only the results from the form factor analysis are presented here. The solid lines are the model fits with cylindrical form factors, which agree with the SANS intensities very well. This clearly indicates that the resulting aggregates obtained by polymerizing CTVB and NaSS mixtures are cylindrical or rodlike particles. The fitting parameters, the length and radius, are summarized in Table 1. Although the radius of the particles is a constant of ∼2 nm for all of the NaSS concentrations, the length varies from 20 to 85 nm, depending on the concentration of NaSS. The radius of the particles is consistent with the stretched chain length of the CTVB tail, 2.18 nm. The fitted values of the polydispersity of the length, p_L, range from 0.32 to 0.42 without showing specific dependency on the NaSS concentration.

Since the structure factor used here is only an approximation which may not be reliable for highly anisotropic charged particles, we performed additional SANS measurements for the higher NaSS molar concentration samples (25 mol % and 40 mol %) at a much lower concentration, 0.01 wt % in D_2O. To minimize the Coulomb interaction between the particles, salt was dissolved in D_2O (0.047 M NaCl). The SANS intensities of 0.01 wt % samples, which show no apparent signatures of the Coulomb interactions, and their model fits with cylindrical form factors are shown in Figure 3b and the fitting parameters are compared with those of 0.1 wt % samples (Table 1). The lengths of the CTVB/NaSS particles determined from 0.01 wt % samples are larger than those determined from 0.1 wt % samples, which is due to the reduced or essentially eliminated interparticle interactions in 0.01 wt % samples. The difference in length, however, is not very big.

Table 1. Results of Model Fit Using the Cylindrical Form Factor and the Guinier Fit of 0.1 and 0.01 wt % Polymerized CTVB/NaSS Particles

	Model fit				Guinier fit		
NaSS (mol %)	radius (nm)	length (nm)	$(\chi^2/N)^{1/2}$	p_L	R_g (nm)	length (nm)	$(\chi^2/N)^{1/2}$
0	1.89 ± 0.003	43.8 ± 0.3	2.9	0.42 ± 0.01	14.3 ± 0.8	49.2 ± 2.7	0.4
5	2.06 ± 0.002	85.0 ± 0.9	5.2	0.33 ± 0.02	21.2 ± 0.6	73.1 ± 2.2	0.6
10	1.87 ± 0.003	50.9 ± 0.4	2.3	0.38 ± 0.01	14.7 ± 0.6	50.6 ± 2.2	0.9
25	1.98 ± 0.002	26.0 ± 0.1	3.9	0.39 ± 0.01	7.6 ± 0.2	26.0 ± 0.7	0.4
	1.90 ± 0.015[a]	28.5 ± 0.6[a]	1.5[a]	0.38 ± 0.01[a]	8.1 ± 0.2[a]	27.6 ± 0.7[a]	1.5[a]
40	1.92 ± 0.002	20.4 ± 0.1	4.3	0.32 ± 0.01	5.9 ± 0.3	19.7 ± 1.1	0.4
	1.99 ± 0.018[a]	24.0 ± 0.5[a]	1.4[a]	0.36 ± 0.01[a]	7.7 ± 0.2[a]	26.2 ± 0.7[a]	1.2[a]

[a] The results from 0.01 wt % polymerized CTVB/NaSS particles in D_2O (0.047 M NaCl).

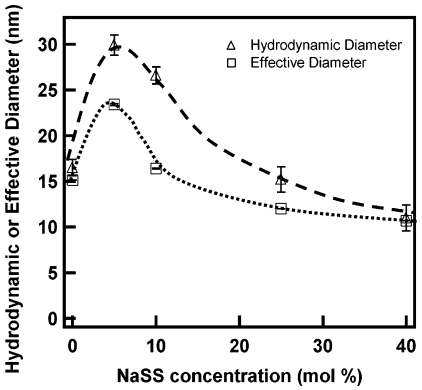

Figure 4. Comparison of hydrodynamic and effective diameter of polymerized CTVB/NaSS particles. The dashed lines are a guide for the eye.

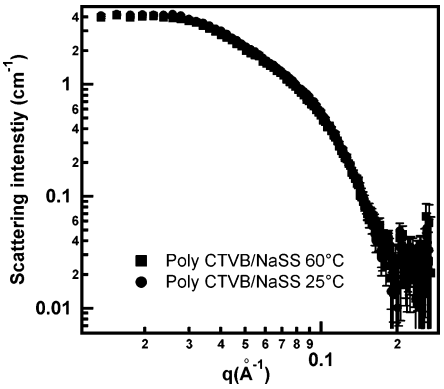

Figure 5. SANS intensity of 1 wt % CTVB/NaSS (40 mol %) after polymerization. The circles are the SANS intensity at 25 °C and the squares are the SANS intensity at 60 °C, showing that the polymerized structures are not temperature sensitive.

The SANS data were also analyzed with the Guinier model to estimate the radius of gyration of the particles. From the radius of gyration, we estimated the length of the rodlike particles using eq 2. Here we used a radius of 2 nm, which was found from the cylindrical form factor analysis at higher q values. The results are summarized in Table 1. The lengths of the rodlike particles estimated from the two independent analyses agree very well. It should be noted that, as the NaSS concentration is increased from zero to 40 mol %, the length of the particles increases initially, and after reaching the maximum at 5 mol %, it decreases monotonically. The size variation of the polymerized CTVB/NaSS particles depending on the NaSS concentration was checked by the DLS measurements of 0.1 wt % polymerized CTVB/NaSS particles. Figure 4 shows that, depending on the NaSS concentration, the hydrodynamic diameter varies from 11.0 to 29.9 nm being peaked at the NaSS concentration of 5 mol %. The polydispersity of hydrodynamic diameter ranges from 0.20 to 0.32 without any explicit dependency on the NaSS concentration. To directly compare the DLS results with the SANS measurements, the effective diameters (D_{eff}) of the CTVB/NaSS particles were calculated from the results of SANS analysis using eq 6. Figure 4 shows that at all of the NaSS concentrations, the effective diameter is smaller than the hydrodynamic diameter, which is understandable considering the definitions of the two diameters. However, the variation of the effective diameters as a function of the NaSS concentrations is consistent with that of the hydrodynamic diameter. This further supports that the estimation of the length and diameter of the rodlike particles from SANS measurements are reliable. The variation of particle length depending on the NaSS concentration can be correlated with the surface charge density of the particles, which will be discussed later.

The equilibrium structure of the micelles and the intermicellar interactions are very sensitive to temperature. The SANS intensities of unpolymerized CTVB micellar solution are strongly influenced by temperature as shown previously.[27] To check the stability of the polymerized particles against temperature change, the SANS measurements of the polymerized CTVB/NaSS particles in D_2O were performed at two different temperatures, 25 and 60 °C. Figure 5 shows that the SANS intensities of 1 wt % polymerized CTVB/NaSS (40 mol %) particles at the two temperatures are essentially identical. This clearly indicates that the polymerized particles are insensitive to temperature variation.

The SANS intensities of 4 wt % polymerized CTVB/NaSS particles in D_2O are shown in Figure 6a. It is clear that the appearance of interaction peaks is strongly dependent on the NaSS concentration. When no NaSS is added, the SANS intensity of polymerized CTVB particles shows a rather broad interaction peak. As the concentration of NaSS is increased to 5 and 10 mol %, the interaction peaks almost completely disappear, resulting in cylindrical form factor like scattering intensities. When the concentration of NaSS is further increased to 40 mol %, however, a clearly pronounced interaction peak at ~0.045 $Å^{-1}$ appears again. Since the concentration of particles was kept constant at 4 wt % in D_2O, the excluded volume interactions between polymerized particles are similar for all of the samples. Therefore, we expect that the change of interaction peaks is induced mainly by the changing Coulomb interactions between the polymerized CTVB/NaSS particles, the strength of which depends on the concentration of NaSS. For the sample without NaSS, if all of the VB^- counterions were polymerized on the surface of the micelles, the resulting polymerized particles were expected to be neutral. However, the corresponding SANS intensity shows a Coulomb interaction peak. This indicates that some of the VB^- counterions may have not been polymerized on the surface of micelles, resulting in slightly positively charged particles. As the NaSS is added, more negatively charged counterions, SS^- ions, become available for copolymerization. When the NaSS concentration is 5 and 10 mol %, the polymerized particles become

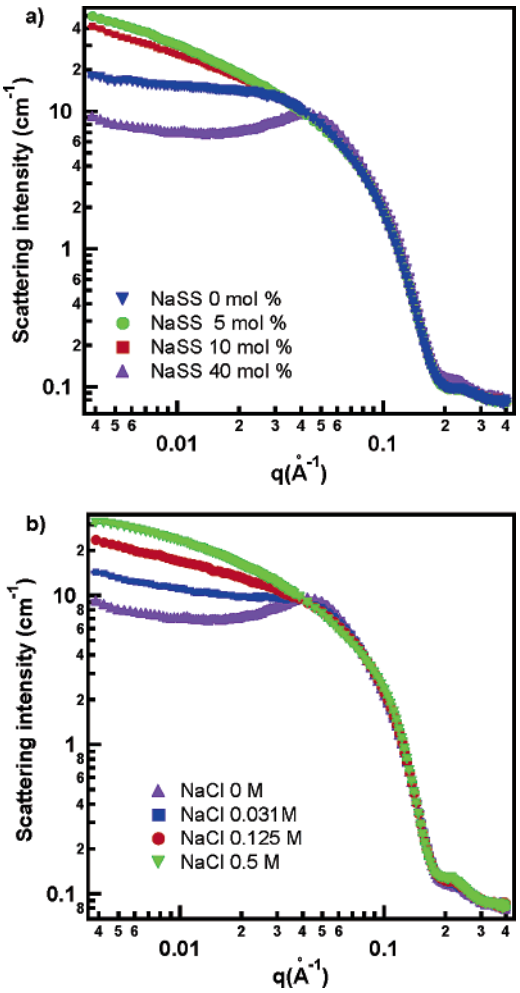

Figure 6. (a) SANS intensities of 4 wt % polymerized CTVB in D_2O with varying NaSS concentrations. The Coulomb interaction peak disappears with increasing NaSS above 5 mol % and reappears at 40 mol % NaSS. Polymerized CTVB without NaSS has a positive charge. (b) Salt (NaCl) screening effect on 4 wt % polymerized CTVB with NaSS 40 mol %. The Coulomb interaction peak disappears as the salt concentration is increased.

more or less neutral, resulting in the cylindrical form factor-like scattering intensities. When the NaSS concentration is increased to 40 mol %, the particles become negatively charged, resulting in the strong Coulomb interaction peak. Nevertheless, the scattered intensities in the high q region overlap for all of the NaSS concentrations, indicating that the cross-sectional structure of the particles is maintained as shown from the form factor analysis of 0.1 wt % samples.

To further confirm that the interaction peaks originate mainly from the Coulomb interaction, a series of SANS measurements of 4 wt % polymerized CTVB/NaSS (40 mol %) particles in D_2O with various NaCl concentrations were performed, shown in Figure 6b. As the NaCl concentration is increased, the interaction peak becomes weaker and, above 0.125 M NaCl concentration, almost completely disappears. This change is due to the salt screening effects and clearly demonstrates that the polymerized CTVB/NaSS (40 mol %) particles are charged.

To quantify the surface charge density of the polymerized CTVB/NaSS rodlike nanoparticles, a series of zeta potential measurements were performed. For these measurements, all of the samples were prepared as 1 wt % particles in D_2O. In this study, the zeta potentials were calculated from the measured electrophoretic mobilities of the CTVB/NaSS particles using the Smoluchowski's equation. For nonconducting cylindrical particles, the Smoluchowski's equation corresponds to the case where all of the cylindrical particles are parallel to the applied electric field.[43] Since the CTVB/NaSS particles may not be parallel to the applied field, however, the zeta potential calculated here may be underestimated. Figure 7 shows that the zeta potential changes from +12.8 to −44.2 mV, as the concentration of NaSS is increased from 0 to 40 mol %. The inset shows the full-width at half-maximum (fwhm) of the measured electrophoretic mobilities from which the fwhm of the zeta potential distributions are estimated. The charge inversion from positive to negative value occurs at the NaSS concentration of about 7 mol %. These results are consistent with the interpretation of the SANS measurements of 4 wt % samples. It should be noted that the zeta potential increases linearly with the NaSS concentration until ~25 mol %, above which it starts to saturate. In general, the overcharging of charged particles by surplus counterions is a spontaneous process to minimize the free energy of the charged particles.[44,45] Once the electrostatic free energy of the charged particles reaches a minimum value, any further amounts of surplus counterions may not contribute to the surface overcharging. To confirm the overcharging limit of polymerized CTVB/NaSS particles, the zeta potentials of the particles with the higher NaSS concentrations (50 and 60 mol %) were measured. The results showed that the zeta potential became saturated to about −50 mV at the NaSS concentration of 60 mol %. It is well-known that multivalent counterions are more effective than monovalent counterions to produce more highly charged particles. Therefore, if multivalent polymerizable counterions are used instead of monovalent SS^- ions, more negatively charged polymerized rodlike particles may be achieved.

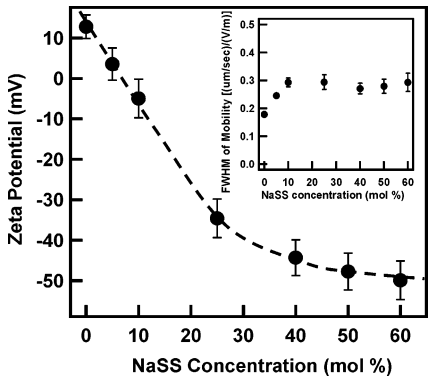

Figure 7. Zeta potentials of polymerized CTVB/NaSS particles with various NaSS concentrations. The zeta potential of polymerized CTVB changes from positive to negative as the concentration of NaSS is increased. Above approximately 25 mol % NaSS, the zeta potential starts to saturate toward a final value of −50 mV. These results are consistent with the results of the SANS measurements. The error bars of the data are the full width half-maximum (fwhm) of zeta potential distribution. The inset shows the fwhm of mobility distribution of the particles. The dashed line is a guide for the eye.

The dependence of the particle length on the NaSS concentration, shown in Table 1, can be understood in terms of the surface charge variation. The electrostatic and repulsive headgroup interactions can be varied by adsorption of counterions, changing the curvature of micelles and hence micellar shape.[1,46] As the surface charge of the micelles increases, the electrostatic repulsions between hydrophilic headgroups dominate and the

(43) Hunter, R. J. *Zeta Potential in Colloid Science*; Academic Press: London, 1981.
(44) Mukherjee, A. K.; Schmitz, K. S.; Bhuiyan, L. B. *Langmuir* **2004**, *20*, 11802.
(45) Mukherjee, A. K.; Schmitz, K. S.; Bhuiyan, L. B. *Langmuir* **2003**, *19*, 9600.
(46) Subramanian, V.; Ducker, W. A. *Langmuir* **2000**, *16*, 4447.

effective headgroup size becomes larger. This results in a larger packing parameter and hence a shorter cylindrical micelle. Therefore, the polymerized CTVB/NaSS particles are shortest when the surface charge density is largest (40 mol % NaSS) and longest when the surface charge density is smallest or nearly zero (5 mol % NaSS).

Conclusion

Rodlike nanoparticles with controlled surface charge density have been developed by the free radical polymerization of a cationic surfactant, cetyltrimethylammonium 4-vinylbenzoate (CTVB), together with varying concentrations of sodium 4-styrenesulfonate (NaSS). The polymerization of the counterions of CTVB which forms wormlike micelle in aqueous solution produces stable rigid rodlike nanoparticles, insensitive to temperature variation. The surface charge density of the rodlike particles was controlled by overcharging the particles with different amounts of NaSS during the polymerization process. The SANS measurements show that the diameter of the polymerized CTVB/NaSS rodlike nanoparticles is constant at 4 nm and the particle length ranges from 24 to 85 nm with polydispersity of 0.33∼0.42, depending on the NaSS concentration. The polymerized particles are longest when the NaSS concentration is 5 mol % which corresponds to the charge inversion or neutral point. The SANS and zeta potential measurements show that the Coulomb interactions between the particles are strongly dependent on the NaSS concentration and the zeta potential of the polymerized CTVB/NaSS nanoparticles changes from positive to negative ($+12.8 \sim -44.2$ mV) as the concentration of NaSS increases from 0 to 40 mol %. As the NaSS concentration was further increased, the zeta potential became saturated at approximately -50 mV. The new techniques developed in this study for preparing rodlike nanoparticles with controlled surface charge density may provide a novel route to producing anisotropic nanoparticles with controlled surface properties that could be used as a building block of new functional nanosystems.

Acknowledgment. This work is supported by the Ministry of Science and Technology of Korea through the Basic Atomic Energy Research Institute (BAERI) program and the HANARO Utilization Project (M2-0411-00-0052), and the Ministry of Health and Welfare of Korea (0405-MN01-0604-007). This work utilized facilities supported in part by the National Science Foundation under Agreement No. DMR-0454672. We thank the HANARO for SANS beamtime supports and Dr. Y. S. Han for technical assistance during SANS measurements.

LA052949A